Intraband Collective Excitations and Spatial Correlations in Fractional Chern Insulators

Tobias Wolf, Yung-Chun Chao, Allan H. MacDonald, and Jung-Jung Su

Phys. Rev. Lett. **134**, 116501 — Published 18 March 2025

DOI: 10.1103/PhysRevLett.134.116501

Intraband collective excitations and spatial correlations in fractional Chern insulators

Tobias Wolf,[1,*] Yung-Chun Chao,[2] Allan H. MacDonald,[1] and Jung-Jung Su[2]
[1]Department of Physics, The University of Texas at Austin, Austin, TX 78712, USA
[2]Department of Electrophysics, National Yang Ming Chiao Tung University, Hsinchu 300, Taiwan
(Dated: February 18, 2025)

The low-energy collective excitations of semiconductors and insulators often couple strongly to light, allowing them to be probed optically. We argue here that in fractional Chern insulators intraband collective excitations are dark in the sense that they couple anomalously weakly to light. Using this property, we establish a general relationship between flat band Chern numbers, quantum geometry, and spatial correlations in fractional Chern insulator states.

PACS numbers: 71.35.-y, 78.67.-n, 73.22.-f

Introduction. The collective excitations of semiconductors and insulators often couple strongly to light, providing both an experimentally convenient probe for fundamental physics studies and a rich axis for optical and electro-optic applications. Optical probes of interband excitonic collective excitations have been especially impactful in transition metal dichalcogenide (TMD) two-dimensional semiconductors [1]. Recently a novel type of insulating state, the fractional Chern insulator (FCI) [2–6], has been discovered in TMD moiré materials [7–10] and in rhombohedral graphene multilayers [11]. Fractional Chern insulators are exotic strongly correlated states with fractionalized quasiparticle excitations that have potential applications in topological quantum computing, and hence are of considerable interest. The appearance of FCI states is thought to be related to weak dispersion of a partially occupied band combined with quantum geometry [12–15] that is suitable in a way that is discussed below. In this paper we argue that FCI's have dark low-energy intraband collective excitations because of their weak band dispersion and spatial correlations similar to those of two-dimensional plasmas because of their quantum geometry.

Dynamic structure factor and optical conductivity. Our conclusions concerning the optical conductivity of fractional Chern insulators follow in part from its relationship to a more general quantity, the dynamic structure factor [16]

$$S(\boldsymbol{q}, E) = \frac{1}{N}\sum_n |\langle \Psi_n|\rho_{\boldsymbol{q}}|\Psi_0\rangle|^2\,\delta(E - E_n + E_0). \quad (1)$$

The static structure factor $S(\boldsymbol{q})$ is the integral of the positive-definite $S(\boldsymbol{q}, E)$ over excitation energy E. In Eq. (1), $|\Psi_n\rangle$ is a many-body eigenstate, the label $n = 0$ is reserved for the ground state, E_n is a many-body energy eigenvalue, $\rho_{\boldsymbol{q}} = \sum_{i=1}^N \rho_{\boldsymbol{q}}^{(i)} = \sum_{i=1}^N \exp(-i\boldsymbol{q}\cdot\hat{\boldsymbol{r}}_i)$ is the density operator and N is the total electron number.

In linear response theory [19], the retarded density-density response function [16]

$$\chi(\boldsymbol{q}, E) = \bar{n}\int_0^\infty dE'\,S(\boldsymbol{q}, E')\Big[\frac{1}{E - E' + i\eta} - \frac{1}{E + E' + i\eta}\Big],$$

where $\bar{n} = N/A$ is the average particle density. To address optical absorption, we consider the real part of the frequency-dependent conductivity σ^{R}_{xx}, which is related to χ by the continuity equation [16],

$$\frac{\sigma^{\mathrm{R}}_{xx}(E)}{E} = -e^2\lim_{q\to 0}\frac{\chi^{\mathrm{I}}(\boldsymbol{q}, E)}{q^2} = \bar{n}\pi e^2\lim_{q\to 0}\frac{S(\boldsymbol{q}, E)}{q^2}, \quad (2)$$

and also related to the current-current response [20, 21] by

$$\sigma^{\mathrm{R}}_{xx}(E) = -\frac{K^{\mathrm{I}}(E)}{E}, \quad (3)$$

where, under the assumption of anisotropy [16],

$$K^{\mathrm{I}}(E) = \frac{1}{A}\sum_n |\langle\Psi_n|j_x|\Psi_0\rangle|^2\,\delta(E - E_n + E_0) \quad (4)$$

and $\boldsymbol{j}$ is the current operator.

Flat band contributions to σ^{R}_{xx}. Our goal is to isolate contributions to the optical conductivity from low-energy transitions within a partially occupied flat band with label f and corresponding Bloch states $|\psi_{f,\boldsymbol{k}}\rangle$. We work to leading order in the ratio of interactions to the energy separation between flat and remote bands, and assume as an inessential convenience that the flat band is lowest in energy. In this limit, we can classify many-body states by the number of electrons in the flat band and identify a low-energy sector in which all electrons occupy the flat band. We note that the flat band contribution to $K^{\mathrm{I}}(E)$ depends only on the band-projected current operator

$$\bar{j}_x = \sum_{\boldsymbol{k}}\langle\psi_{f,\boldsymbol{k}}|j_x|\psi_{f,\boldsymbol{k}}\rangle\, a^\dagger_{f,\boldsymbol{k}}a_{f,\boldsymbol{k}} = -e\sum_{\boldsymbol{k}}(v_x)_{f,\boldsymbol{k}}\, a^\dagger_{f,\boldsymbol{k}}a_{f,\boldsymbol{k}}, \quad (5)$$

where $\boldsymbol{v}_{f,\boldsymbol{k}} = \hbar^{-1}\nabla_{\boldsymbol{k}}\epsilon_{f,\boldsymbol{k}}$ is the band velocity and the operators $a^{(\dagger)}_{f,\boldsymbol{k}}$ destroy (create) the corresponding Bloch states. Since the band velocity $\boldsymbol{v}_{f,\boldsymbol{k}}$ vanishes for a perfectly flat band, it follows that the flat-band contribution to $K^{\mathrm{I}}(E)$, and thus to $\sigma^{\mathrm{R}}_{xx}(E)$ and $S(\boldsymbol{q}, E)/q^2$, vanishes in the same limit.

Flat band contributions to $S(\boldsymbol{q})$. We introduce the flat-band Bloch state projector $P_{f,\boldsymbol{k}} = |\psi_{f,\boldsymbol{k}}\rangle\langle\psi_{f,\boldsymbol{k}}|$ and consider the projected density $\bar{\rho}^{(i)}_{\boldsymbol{q}} = \sum_{\boldsymbol{k}\in\mathrm{BZ}} P^{(i)}_{f,\boldsymbol{k}-\boldsymbol{q}}\, e^{-i\boldsymbol{q}\cdot\hat{\boldsymbol{r}}_i}\, P^{(i)}_{f,\boldsymbol{k}}$ with corresponding projected dynamic structure factor

$$\bar{S}(\boldsymbol{q}, E) = \frac{1}{N}\sum_n |\langle\Psi_n|\bar{\rho}_{\boldsymbol{q}}|\Psi_0\rangle|^2\,\delta(E - E_n + E_0). \quad (6)$$

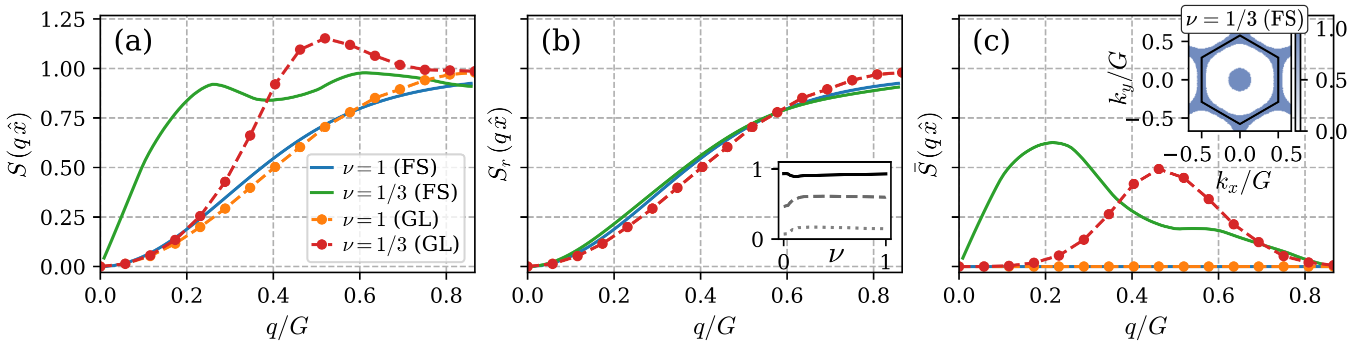

FIG. 1. Total, remote band, and projected static structure factors for Fermi sea (FS) states, and generalized Laughlin (GL) states [cf. Eq. (12)] as particular candidate FCI state. (a) The total structure factor $S(q\,\hat{x})$ at fractional band filling $\nu = 1/3$ behaves like q^2 at long wavelength in insulating states but like q in Fermi liquid states. Corresponding $\nu = 1$ structure factors are shown for comparison. (b) The remote band structure factor $S_{\mathrm{r}}(q\,\hat{x})$ of Fermi sea states and generalized Laughlin states at $\nu = 1$ and $\nu = 1/3$. The inset shows the filling factor dependence $S_{\mathrm{r}}(q'\,\hat{x})$ *vs.* ν for the Fermi sea states at select momenta $q'/(\sqrt{3}G/2) = 0.2, 0.5, 1.0$ (dotted, dashed, and solid lines). (c) The projected static structure factor $\bar{S}(q\,\hat{x})$ vanishes as q^4 for generalized Laughlin states but as q for Fermi liquid states. The inset shows the occupation of the FS state at $\nu = 1/3$ in the first Brillouin zone. The FS states here are for partially-filled, near-flat bands with near-ideal quantum geometry obtained from the moiré homobilayer $MoTe_2$ continuum model at twist angle $\theta = 3°$ with reciprocal lattice constant $G = 4\pi/(\sqrt{3}a_{\mathrm{M}})$, see Ref. [16].

The projected static structure factor $\bar{S}(\boldsymbol{q})$ (the integral of the positive-definite $\bar{S}(\boldsymbol{q}, E)$ over E) is a measure of the density response within the flat band sector, and the coefficient of q^2 in its long-wavelength limit a measure of its contribution to the optical conductivity [cf. Eq. (2)]. As explained above, this quantity vanishes in the case of perfectly flat bands.

Remote band contributions to $S(\boldsymbol{q})$ and ideal quantum geometry. To separate the flat-band projected contribution from the full $S(\boldsymbol{q})$, we note that [16]

$$S(\boldsymbol{q}) \equiv \frac{1}{N}\langle \rho_{-\boldsymbol{q}}\rho_{\boldsymbol{q}}\rangle_0 = \frac{1}{N}\sum_{ij}\langle e^{i\boldsymbol{q}\cdot\hat{\boldsymbol{r}}_i} e^{-i\boldsymbol{q}\cdot\hat{\boldsymbol{r}}_j}\rangle \tag{7}$$

has same ($i = j$) and distinct ($i \neq j$) particle contributions, and that band-projection is relevant only for the former [22]:

$$S_{ii}(\boldsymbol{q}) = \frac{1}{N}\sum_{b\boldsymbol{k}}\langle u_{f,\boldsymbol{k}}|u_{b,\boldsymbol{k}+\boldsymbol{q}}\rangle\,\langle u_{b,\boldsymbol{k}+\boldsymbol{q}}|u_{f,\boldsymbol{k}}\rangle\,\langle n_{f,\boldsymbol{k}}\rangle,$$

where b labels band indices, $\langle \boldsymbol{r}|u_{b,\boldsymbol{k}}\rangle = e^{-i\boldsymbol{k}\cdot\boldsymbol{r}}\langle \boldsymbol{r}|\psi_{b,\boldsymbol{k}}\rangle$ is the periodic part of the Bloch state, and $n_{f,\boldsymbol{k}} = a^\dagger_{f,\boldsymbol{k}}a_{f,\boldsymbol{k}}$ is the occupation operator. The projected static structure differs only in that band summation is restricted to $b = f$, such that

$$S_{\mathrm{r}}(\boldsymbol{q}) = S(\boldsymbol{q}) - \bar{S}(\boldsymbol{q}) = \sum_{\boldsymbol{k}}\left[1 - |\langle u_{f,\boldsymbol{k}+\boldsymbol{q}}|u_{f,\boldsymbol{k}}\rangle|^2\right]\frac{\langle n_{f,\boldsymbol{k}}\rangle}{N} \tag{8}$$

is the remote band contribution to the static structure factor. Note that Eqs. (1) and (6) imply that $S_{\mathrm{r}}(\boldsymbol{q}, E) \leq S(\boldsymbol{q}, E)$; a corresponding inequality extends to the static structure factors by integrating over E. For flat-band insulating states, the inequality is saturated to order q^2 in the long-wavelength limit due to the absence of a flat-band contribution. A similar inequality has recently been discussed in Ref. [23].

At long-wavelengths, Eq. (8) relates the remote-band structure factor $S_{\mathrm{r}}(\boldsymbol{q})$ to the Fubini-Study tensor integrated over the Brillouin-zone and weighted by band occupations:

$$\lim_{q\to 0} S_{\mathrm{r}}(\boldsymbol{q}) = q_\mu q_\nu \frac{1}{N}\sum_{\boldsymbol{k}}\left(g_{f,\boldsymbol{k}}\right)_{\mu\nu}\,\langle n_{f,\boldsymbol{k}}\rangle, \tag{9}$$

where $|\langle u_{b,\boldsymbol{k}-d\boldsymbol{q}}|u_{b,\boldsymbol{k}}\rangle|^2 = 1 - \left(g_{b,\boldsymbol{k}}\right)_{\mu\nu} dq_\mu dq_\nu$ with an implied sum over μ, ν defines the Fubini-Study tensor $g_{b,\boldsymbol{k}}$ [12]. We comment below that the band states are equally occupied in insulating states at fractional band fillings. Eq. (9) implies that $S_{\mathrm{r}}(\boldsymbol{q})$ vanishes at least quadratically in q for any many-body state. When a band possesses the Landau-level-like *ideal quantum geometry* thought to be associated with FCI states, the quadratic coefficient in Eq. (9) is tied to the Chern number: if (A) the ground state band-occupation numbers $\langle n_{f,\boldsymbol{k}}\rangle$ are $\boldsymbol{k}$-independent, (B) the ideal quantum geometry trace condition $\mathrm{tr}[g_{f,\boldsymbol{k}}] = \Omega_{f,\boldsymbol{k}}$ holds ($\Omega_{f,\boldsymbol{k}}$ is the Berry curvature), and (C) the system has sufficient symmetries such that $\sum_{\boldsymbol{k}} g_{f,\boldsymbol{k}}$ is proportional to the identity matrix, then Eq. (9) leads to [16]

$$\lim_{q\to 0}\frac{S_{\mathrm{r}}(\boldsymbol{q})}{q^2} = |C_f|\,\frac{A_0}{4\pi} = \frac{A_0}{4\pi}, \tag{10}$$

where $|C_f| = 1$ is the Chern number of band f.

We have so far argued that the static and dynamic structure factors can be partitioned into flat and remote band contributions, and that for insulating states at fractional filling factors the flat band is absent to order q^2 and the remote band fixed by band Chern number. Figure 1 illustrates expected properties of the partitioned structure factor for moiré homobilayer $MoTe_2$ [16], the prime experimental example of FCI states. In realistic cases the flat bands are never perfectly dispersionless and Fermi liquid states can therefore be established at fractional filling factors if interactions are sufficiently weak. Figure 1 compares the full, remote-band, and projected structure factors of Fermi liquid and FCI states. For the FCI states the structure factor has been calculated using a generalized Laughlin variational state discussed below. Although $S_{\mathrm{r}}(\boldsymbol{q})$ is similar in the two cases, the full static structure factors $S(\boldsymbol{q})$ differ strongly, and the flat-band contribution even more strongly. For flat-band FCI states, $\bar{S}(\boldsymbol{q})$ vanishes quartically in q, in comparison to the quadratic behavior of generic insulators and the linear behavior of Fermi liquids, which is related to its gapless excitations. (When the weak band dispersion of realistic FCI states is included the coefficient of q^2 in $\bar{S}(\boldsymbol{q})$ is non-zero but proportional to the small parameter W/Δ, where W is the flat-band width and Δ is the FCI gap.)

Generalized Laughlin states, plasma analogy and perfect screening. It follows the absence of a flat band contribution to order q^2 that the full static structure factor also satisfies Eq. (10). Expanding Eq. (7) to order q^2 and comparing with Eq. (10) it follows that

$$\int_{A_0} d^2\boldsymbol{r} \int_A d^2\boldsymbol{r}' |\boldsymbol{r}-\boldsymbol{r}'|^2 [n^2(\boldsymbol{r},\boldsymbol{r}') - n(\boldsymbol{r})n(\boldsymbol{r}')] = \frac{A_0}{2\pi} \quad (11)$$

for any flat band FCI state. This second moment sum rule for pair correlation functions $n^2(\boldsymbol{r},\boldsymbol{r}') - n(\boldsymbol{r})n(\boldsymbol{r}')$ of FCI states is shared with two-dimensional classical plasmas [24] and can be established by an instructive alternate argument in the special case of short-range interactions and band filling $\nu = 1/m$ (odd m). In that case the incompressible ground states [12, 14, 25] are generalized Laughlin many-body states [16, 26]. The N-particle wavefunction in real-space coordinates is

$$\Psi_m(\boldsymbol{r}_1,\ldots,\boldsymbol{r}_N) = \prod_{i<j}^{N} (z_i - z_j)^m \prod_{k=1}^{N} e^{-\frac{|z_k|^2}{4\ell^2} + \Phi(\boldsymbol{r}_k)}, \quad (12)$$

where $z_k = x_k + iy_k$ is position expressed as a complex number, ℓ is the magnetic length corresponding to a quantum of pseudo magnetic field [32] per unit cell area A_0 (i.e., $2\pi\ell^2 = A_0$), and $\Phi(\boldsymbol{r})$ is a periodic function with zero average value that distinguishes one ideal flat band from another.

The wavefunction Ψ_m is a product of polynomial and Gaussian factors that respectively increase and decrease in magnitude exponentially with N; the factors must balance in order for $|\Psi_m|^2$ to have a sensible thermodynamic limit, implying $mN = N_{\mathrm{uc}}$, where $N_{\mathrm{uc}} = A/A_0$ is the number of moiré periods in the system. To make this argument, we can view $|\Psi_m|^2 \propto \exp(-U(\boldsymbol{r}_1,\ldots,\boldsymbol{r}_N)/m)$ as the classical Boltzmann weight of a 2D Coulomb plasma [33] with particles of charge $q_i = m$. With this identification, Eq. (12) leads to

$$U = -\sum_{i=1}^{N} q_i \phi_{\mathrm{b}}(\boldsymbol{r}_i) + \sum_{i<j}^{N} q_i V(\boldsymbol{r}_i - \boldsymbol{r}_j) q_j, \quad (13)$$

where $V(\boldsymbol{r}) \equiv -2\ln|\boldsymbol{r}|$ and $\phi_{\mathrm{b}}(\boldsymbol{r}) = \int d^2r'\, V(\boldsymbol{r}-\boldsymbol{r}')\, \rho_{\mathrm{b}}(\boldsymbol{r}')$ is the attractive 2D Coulomb potential produced by the background charge $\rho_{\mathrm{b}}(\boldsymbol{r}) = (2\pi\ell^2)^{-1} - \nabla^2\Phi(\boldsymbol{r})/2\pi \equiv A^{-1} \cdot \sum_{\boldsymbol{G}} e^{i\boldsymbol{G}\cdot\boldsymbol{r}} \rho_{\mathrm{b}\boldsymbol{G}}$ with $\rho_{\mathrm{b}\boldsymbol{0}} = A/(2\pi\ell^2)$ [34]. The plasma distribution function has a sensible thermodynamic limit only when it is charge neutral ($\rho_{\mathrm{b}\boldsymbol{0}} = m\rho_{\boldsymbol{0}} = mN$), capturing the constraint $mN = N_{\mathrm{uc}}$. The average particle density then is

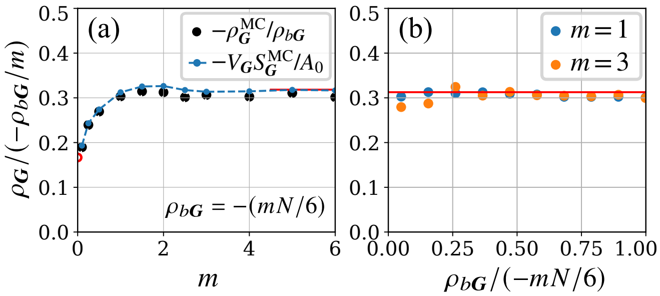

FIG. 2. Dependence of the first reciprocal lattice vector shell charge density modulation $\rho_{\boldsymbol{G}}$ on the plasma coupling parameter m and the background modulation $\rho_{\mathrm{b}\boldsymbol{G}}$. (a) Dependence of the $\rho_{\boldsymbol{G}}$ calculated by sampling the plasma distribution function on the plasma coupling parameter m. The exact charge modulation (black) is well-described by the linear response relation (blue) when Monte-Carlo results are used for the unperturbed system structure factor, and agrees with analytical results in the limiting cases $m \to 0$ and $m \gg 1$ (red). (b) Dependence of $\rho_{\boldsymbol{G}}$ on background density modulation $\rho_{\mathrm{b}\boldsymbol{G}}$ a$m = 1$ and $m = 3$, showing that all considered background modulations are well within the linear response regime.

$\bar{n} = N/A = (m2\pi\ell^2)^{-1} = 1/(mA_0)$, implying that the band filling factor for this state is $\nu = 1/m$. For the calculations we describe below it is convenient to write U in momentum space using $\rho_{\boldsymbol{k}} = \sum_i e^{-\boldsymbol{k}\cdot\boldsymbol{r}_i}$, such that

$$U = \frac{1}{2A} \sum_{\boldsymbol{k}\neq 0} \frac{4\pi}{|\boldsymbol{k}|^2} \, |m\rho_{\boldsymbol{k}} - \rho_{\mathrm{b}\boldsymbol{k}}|^2, \quad (14)$$

up to constant terms that do not change the relative weight.

Next we argue that the average density in any region much larger than one unit cell must approach ν/A_0 even when one particle is held fixed near the center of that region. In the plasma analogy this is known as Stillinger-Lovett perfect screening [24, 35, 36], which implies that the plasma inverse dielectric function vanishes at long wavelengths:

$$\epsilon^{-1}(\boldsymbol{q}) = 1 + \frac{4\pi m}{q^2}\chi(\boldsymbol{q}) \underset{q\to 0}{\longrightarrow} 0. \quad (15)$$

Since the plasma response function $\chi(\boldsymbol{q})$ and $S(\boldsymbol{q})$ are both Fourier transforms of the two-particle density correlation function (up to normalization), Eq. (15) implies

$$\lim_{q\to 0} \frac{S(\boldsymbol{q})}{q^2} = \frac{\ell^2}{2} = \frac{A_0}{4\pi}, \quad (16)$$

and thus leads to the same quadratic coefficient as in Eq. (10). Thus combining the ideal band condition Eq. (10) with generalized Laughlin incompressible state wavefunctions leads to the same conclusion as combining it with the assumption of perfectly flat-bands: the dipole contribution to $S(\boldsymbol{q})$ is exhausted by the remote-band response, leaving no room for a flat-band contributions.

Eq. (10) applies when band occupation probabilities $\langle n_{f,\boldsymbol{k}}\rangle$ are $\boldsymbol{k}$-independent for Ψ_m not just for the filled band, $m = 1$, but for any fractional filling $m > 1$. The argument has two ingredients: (i) band vortexibility [14] together with the density matrix properties in Ref. [37] non-trivially implies that two vortexable band states with proportional charge densities have proportional one-particle density matrices [37], and thus since

$$\langle n_{f,\boldsymbol{k}}\rangle = \int d^2r d^2r'\, \psi^*_{f,\boldsymbol{k}}(\boldsymbol{r})\, \rho^{(1)}(\boldsymbol{r},\boldsymbol{r}')\, \psi_{f,\boldsymbol{k}}(\boldsymbol{r}') \tag{17}$$

proportional occupation numbers; and (ii) that the charge density of a generalized Laughlin state ($m > 1$) is approximately $1/m$ times the charge density of a filled flat band ($m = 1$). (In the SM [16] we provide an alternative proof that $n_{f,\boldsymbol{k}}$ is constant (Sec. IV.B) and Eq. (10) holds (Sec. IV.D).) In the presence of weak band dispersion the generalized Laughlin states are no longer exact ground states, lower-energy band states will have slightly higher occupation than higher-energy band states and the parametrically small current response to electric fields is achieved by differential occupation of states with velocities of opposite sign.

Plasma gas and local background cancellation. To establish property (ii) using the plasma analogy, we calculate the m-dependence of the Fourier components of the charge density $\langle\rho_{\boldsymbol{k}}\rangle = \langle\Psi_m|\rho_{\boldsymbol{k}}|\Psi_m\rangle$ by Monte-Carlo sampling of the plasma analogy Boltzmann distribution in Eq. (14), see [16] for details. In linear response [16], the induced charge density at wavevector $\boldsymbol{G}$ is proportional to the background charge density at that wavevector and to the static structure factor of the unperturbed uniform system:

$$\langle\rho_{\boldsymbol{G}}\rangle = -\frac{1}{A_0}\frac{4\pi}{|\boldsymbol{G}|^2} S(\boldsymbol{G})\bigg|_{\rho_{\mathrm{b}\boldsymbol{G}}=0} \frac{\rho_{\mathrm{b}\boldsymbol{G}}}{m}. \tag{18}$$

To see how Eq. (18) justifies property (ii), we note that the density $\bar{n} = 1/(mA_0)$ sets the natural length scale for the structure factor $S(\boldsymbol{q})$: For the first shell, $|\boldsymbol{G}|\,\bar{n}^{-1/2} = (8\pi^2 m/\sqrt{3})^{1/2} \approx 6.75\sqrt{m}$ is large already at $m = 1$ which leads to uncorrelated values $S(\boldsymbol{G}) \approx 1$. For $m \geq 1$, we thus estimate $\langle\rho_{\boldsymbol{G}}\rangle \approx -(4\pi/A_0|\boldsymbol{G}|^2)(\rho_{\mathrm{b}\boldsymbol{G}}/m) = -\sqrt{3}/(2\pi)(\rho_{\mathrm{b}\boldsymbol{G}}/m) \approx -0.05N$. In Fig. 2, we show the first-shell charge density $\rho_{\boldsymbol{G}}$ *vs.* m in the presence of a non-uniform background charge, obtained using Monte Carlo to sample the plasma distribution [16]. We find that calculating $\rho_{\boldsymbol{G}}$ by sampling the non-uniform system gives the same results as Eq. (18) with the uniform system correlation function. In the regime of positive definite background charge density studied here, our calculations verify the accuracy of Eq. (18). We further remark that for $m \to 0$, $|\boldsymbol{G}|\,\bar{n}^{-1/2}$ is small, justifying the perfect screening limit of Eq. (16). This yields $m\rho_{\boldsymbol{G}} = -\rho_{\mathrm{b}\boldsymbol{G}}$, also in agreement with direct Monte-Carlo evaluation, see Fig. 2. For $m \to 0$, the charge density thus locally cancels the background density, and becomes insensitive to plasma interactions. On physical grounds, we expect that the result for both limits survive into the non-linear regime of more strongly varying charge densities. Importantly for this work, we found property (ii): at fractional filling $\nu = 1/m$ the charge density [by (i) also the band occupation] is simply $1/m$ times that of the filled-band.

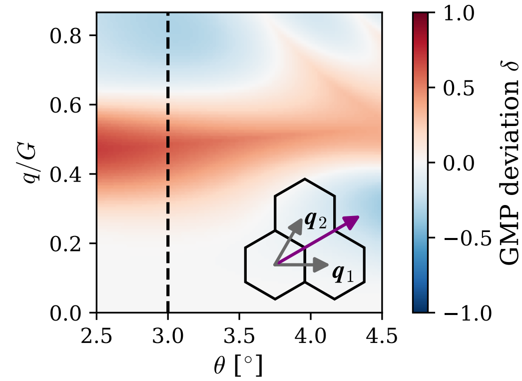

FIG. 3. GMP algebra deviation $\delta(q)$ of the projected structure factor in the nearly-flat moiré valence band of homobilayer $MoTe_2$ as function of twist angle θ. We quantify the violation by defining $\delta(q) \equiv |\langle\psi_{f,\boldsymbol{k}+\boldsymbol{q}_1+\boldsymbol{q}_2}|\left[\rho_{\boldsymbol{q}_1},\rho_{\boldsymbol{q}_2}\right]|\psi_{f,\boldsymbol{k}}\rangle| - |\langle\psi_{f,\boldsymbol{k}+\boldsymbol{q}_1+\boldsymbol{q}_2}|2i\sin(\boldsymbol{q}_1\wedge\boldsymbol{q}_2\cdot\boldsymbol{\Omega}(\boldsymbol{k})/2)\,\rho_{\boldsymbol{q}_1+\boldsymbol{q}_2}\,|\psi_{f,\boldsymbol{k}}\rangle|$ with $\boldsymbol{k} = 0$ and $\boldsymbol{q}_1, \boldsymbol{q}_2$ as indicated in the inset ($|\boldsymbol{q}_1| = |\boldsymbol{q}_2| = q$). The highlighted angle $\theta = 3°$ has both the smallest flatband width and smallest trace condition deviation. See Ref. [16] for details on the continuum model.

Discussion. We have shown that dipole transitions within a $|C| = 1$ flat ideal band are parametrically weak. This property of ideal Chern bands is shared with Landau bands, in which dipole transitions are entirely inter-Landau level by virtue of Kohn's theorem [38]. It is natural to examine the degree to which the two cases are similar at larger momentum. The properties of density response functions within a Landau level are constrained by the GMP algebra [39] of projected density operators.

$$[\bar\rho_{\boldsymbol{q}_1},\bar\rho_{\boldsymbol{q}_2}] = 2i\,\sin(\boldsymbol{q}_1\wedge\boldsymbol{q}_2\ell^2/2)\,e^{\boldsymbol{q}_1\cdot\boldsymbol{q}_2\ell^2/2}\,\bar\rho_{\boldsymbol{q}_1+\boldsymbol{q}_2}. \tag{19}$$

The corresponding operator projected to a Chern band maps Brillouin zone momentum $\boldsymbol{k}$ to $\boldsymbol{k}+\boldsymbol{q}_1+\boldsymbol{q}_2$ as in the Landau level case, but with a coefficient that depends on the starting $\boldsymbol{k}$:

$$\begin{aligned}&\langle\psi_{\boldsymbol{k}+\boldsymbol{q}_1+\boldsymbol{q}_2}|[\bar\rho_{\boldsymbol{q}_1},\bar\rho_{\boldsymbol{q}_2}]|\psi_{\boldsymbol{k}}\rangle = \\ &\quad\langle u_{\boldsymbol{k}+\boldsymbol{q}_1+\boldsymbol{q}_2}|u_{\boldsymbol{k}+\boldsymbol{q}_2}\rangle\langle u_{\boldsymbol{k}+\boldsymbol{q}_2}|u_{\boldsymbol{k}}\rangle - \langle u_{\boldsymbol{k}+\boldsymbol{q}_1+\boldsymbol{q}_2}|u_{\boldsymbol{k}+\boldsymbol{q}_1}\rangle\langle u_{\boldsymbol{k}+\boldsymbol{q}_1}|u_{\boldsymbol{k}}\rangle,\end{aligned} \tag{20}$$

where we omitted the band label for brevity and note that $|u_{\boldsymbol{k}'}\rangle = e^{-i\boldsymbol{g}\cdot\hat{\boldsymbol{r}}}\,|u_{\lfloor\boldsymbol{k}'\rfloor}\rangle$ with momenta $\lfloor\boldsymbol{k}'\rfloor = \boldsymbol{k}' - \boldsymbol{g}$ reduced to the first Brillouin zone [22]. The deviation of the projected density operator matrix elements from GMP algebra values is shown in Fig. 3 as a function of $|\boldsymbol{q}_1|$ and twist angle for $|\boldsymbol{q}_1| = |\boldsymbol{q}_2|$ and a 60° angle between the two wavevectors. These calculations are for the same model of $MoTe_2$ homobilayer moirés used to produce the Fermi liquid structure factors in Fig. 1 for the twist angle $\theta \approx 3°$ at which ideal quantum geometry is most closely approached. We see in Fig. 3 that the GMP algebra is approximately satisfied for small $\boldsymbol{q}$ over a wide range of twist angles surrounding the most ideal one, and that the agreement with GMP algebra is poor at large $\boldsymbol{q}$. These results suggest that optical matrix elements will have a strong tendency to be suppressed in Chern bands even if they are relatively far from ideal - and perhaps that the interaction physics responsible for the fractional quantum anomalous Hall effect, which is most easily explained when bands are prefectly ideal, is also tolerant to deviations [40].

Although dipole allowed transitions are exceptionally weak for intraband excitations, the oscillator strengths are not precisely zero, there is some hope that optical probes will still prove useful. We do expect intraband oscillator strengths to increase with disorder and flat band width, just as in the non-anomalous strong-mangetic-field fractional quantum Hall effect [37, 41, 42]. while remaining a small part of the full f-sum rule weight. The larger interband absorption signals can also provide useful insights and will likely reveal the small ratio between neutral and charged interband excitation energies that is familiar from ordinary fractional quantum Hall systems.

The conclusions of this paper are intended to apply rather broadly to fractional Chern insulator states, although we have performed specific calculations for a model of TMD AA moiré homobilayers [43], the system in which FCI states have recently been observed. In real systems like this, ideal quantum geometry will never be perfectly realized. Nearly ideal quantum geometry is however apparently sufficient for Landau-level-like correlations at long length scales, as characterized for example by the density-matrix properties summarized in Fig. 3.

Acknowledgments. This work was supported by the Simons Foundation and the Welch Foundation. Y.-C.C and J.-J.S acknowledge the support from Ministry of Science and Technology, Taiwan 112-2112-M-A49-039, 110-2124-M-A49 -008 -MY3 and Center for Theoretical and Computational Physics (CTCP) of NYCU.

* tobias.wolf@austin.utexas.edu

[1] G. Wang, A. Chernikov, M. M. Glazov, T. F. Heinz, X. Marie, T. Amand, and B. Urbaszek, Colloquium: Excitons in atomically thin transition metal dichalcogenides, Rev. Mod. Phys. **90**, 021001 (2018).

[2] E. Tang, J.-W. Mei, and X.-G. Wen, High-temperature fractional quantum hall states, Phys. Rev. Lett. **106**, 236802 (2011).

[3] H. Li, U. Kumar, K. Sun, and S.-Z. Lin, Spontaneous fractional chern insulators in transition metal dichalcogenide moiré superlattices, Phys. Rev. Research **3**, L032070 (2021).

[4] T. Neupert, L. Santos, C. Chamon, and C. Mudry, Fractional quantum hall states at zero magnetic field, Phys. Rev. Lett. **106**, 236804 (2011).

[5] N. Regnault and B. A. Bernevig, Fractional chern insulator, Phys. Rev. X **1**, 021014 (2011).

[6] D. N. Sheng, Z.-C. Gu, K. Sun, and L. Sheng, Fractional quantum hall effect in the absence of landau levels, Nat. Commun. **2**, 389 (2011).

[7] J. Cai, E. Anderson, C. Wang, X. Zhang, X. Liu, W. Holtzmann, Y. Zhang, F. Fan, T. Taniguchi, K. Watanabe, *et al.*, Signatures of fractional quantum anomalous Hall states in twisted $MoTe_2$, Nature **622**, 63 (2023).

[8] Y. Zeng, Z. Xia, K. Kang, J. Zhu, P. Knüppel, C. Vaswani, K. Watanabe, T. Taniguchi, K. F. Mak, and J. Shan, Thermodynamic evidence of fractional Chern insulator in moiré $MoTe_2$, Nature **622**, 69 (2023).

[9] H. Park, J. Cai, E. Anderson, Y. Zhang, J. Zhu, X. Liu, C. Wang, W. Holtzmann, C. Hu, Z. Liu, *et al.*, Observation of fractionally quantized anomalous Hall effect, Nature **622**, 74 (2023).

[10] F. Xu, Z. Sun, T. Jia, C. Liu, C. Xu, C. Li, Y. Gu, K. Watanabe, T. Taniguchi, B. Tong, J. Jia, Z. Shi, S. Jiang, Y. Zhang, X. Liu, and T. Li, Observation of integer and fractional quantum anomalous Hall effects in twisted bilayer $MoTe_2$, Phys. Rev. X **13**, 031037 (2023).

[11] Z. Lu, T. Han, Y. Yao, A. P. Reddy, J. Yang, J. Seo, K. Watanabe, T. Taniguchi, L. Fu, and L. Ju, Fractional quantum anomalous hall effect in multilayer graphene, Nature **626**, 759 (2024).

[12] R. Roy, Band geometry of fractional topological insulators, Phys. Rev. B **90**, 165139 (2014).

[13] S. A. Parameswaran, R. Roy, and S. L. Sondhi, Fractional chern insulators and the W_∞ algebra, Phys. Rev. B **85**, 241308 (2012).

[14] P. J. Ledwith, A. Vishwanath, and D. E. Parker, Vortexability: A unifying criterion for ideal fractional Chern insulators, Phys. Rev. B **108**, 205144 (2023).

[15] There is experimental evidence that the ideal-quantum-geometry (Aharonov-Casher-band) fractional-Chern-insulator scenario applies to WTe_2: for the observed state, the fractional Hall conductivity quantum number equals the fractional band filling factor. The same property is found in FQAHE experiments with graphene multilayers. Our analysis applies to this FQAHE scenario, but future experiments in other regimes or materials may feature different mechanisms.

[16] See Supplemental Material for (I) details on the continuum model for homobilayer moiré TMDs, (II) details on the structure factor and response functions (including finite temperature definitions), as well as (III) the generalized Laughlin wavefunction and its relation to vortexible Chern-1 bands, the plasma analogy and Monte-Carlo importance sampling; it includes Refs. [17, 18].

[17] C. Wang, X.-W. Zhang, X. Liu, Y. He, X. Xu, Y. Ran, T. Cao, and D. Xiao, Fractional chern insulator in twisted bilayer $mote_2$, Phys. Rev. Lett. **132**, 036501 (2024).

[18] Y. Aharonov and A. Casher, Ground state of a spin-1/2 charged particle in a two-dimensional magnetic field, Physical Review A **19**, 2461 (1979).

[19] In a system with the discrete translation symmetry of a crystal the density-density response is non-zero when its momentum arguments differ by reciprocal lattice vectors. The χ and S referred to here are diagonal elements of the response matrix.

[20] G. Giuliani and G. Vignale, *Quantum theory of the electron liquid* (Cambridge university press, 2008).

[21] G. D. Mahan, *Many-particle physics* (Springer Science & Business Media, 2013).

[22] See Eq. (S16) in the Supplemental Material [16] for details on the first Brillouin zone mapping of inner products.

[23] Y. Onishi and L. Fu, Fundamental bound on topological gap, Phys. Rev. X **14**, 011052 (2024).

[24] P. J. Forrester, *Log-gases and random matrices (LMS-34)* (Princeton university press, 2010).

[25] J. Wang, J. Cano, A. J. Millis, Z. Liu, and B. Yang, Exact landau level description of geometry and interaction in a flatband, Phys. Rev. Lett. **127**, 246403 (2021).

[26] While not yet established experimentally, there are strong arguments [27–32] that this connection to quantum geometry applies to all moiré material FCI states. The 'flatness' of the band dispersion seemingly plays no role in affecting properties of Ψ_m – but note that the argument that Ψ_m is the ground state will break down in presence of significant band dispersion.

[27] N. Morales-Durán, J. Wang, G. R. Schleder, M. Angeli, Z. Zhu, E. Kaxiras, C. Repellin, and J. Cano, Pressure-enhanced fractional chern insulators along a magic line in moiré transition

metal dichalcogenides, Phys. Rev. Research **5**, L032022 (2023).
[28] J. Shi, N. Morales-Durán, E. Khalaf, and A. H. MacDonald, Adiabatic approximation and aharonov-casher bands in twisted homobilayer tmds (2024), arXiv:2404.13455 [cond-mat.mes-hall].
[29] B. Li and F. Wu, Variational mapping of chern bands to landau levels: Application to fractional chern insulators in twisted mote$_2$ (2024), arXiv:2405.20307 [cond-mat.mes-hall].
[30] J. Wang, S. Klevtsov, and Z. Liu, Origin of model fractional chern insulators in all topological ideal flatbands: Explicit color-entangled wave function and exact density algebra, Phys. Rev. Res. **5**, 023167 (2023).
[31] M. Fujimoto, D. E. Parker, J. Dong, E. Khalaf, A. Vishwanath, and P. Ledwith, Higher vortexability: zero field realization of higher landau levels (2024), arXiv:2403.00856 [cond-mat.mes-hall].
[32] N. Morales-Durán, N. Wei, J. Shi, and A. H. MacDonald, Magic angles and fractional chern insulators in twisted homobilayer transition metal dichalcogenides, Physical Review Letters **132**, 096602 (2024).
[33] R. B. Laughlin, Anomalous quantum hall effect: An incompressible quantum fluid with fractionally charged excitations, Phys. Rev. Lett. **50**, 1395 (1983).
[34] Since $\nabla^2\Phi(\boldsymbol{r})$ is periodic, it does not contribute to the total plasma density.
[35] F. H. Stillinger Jr and R. Lovett, General restriction on the distribution of ions in electrolytes, J. Chem. Phys. **49**, 1991 (1968).
[36] F. H. Stillinger Jr and R. Lovett, Ion-pair theory of concentrated electrolytes. i. basic concepts, J. Chem. Phys. **48**, 3858 (1968).
[37] A. MacDonald and S. Girvin, Density matrices for states in the lowest landau level of a two-dimensional electron gas, Phys. Rev. B **38**, 6295 (1988).
[38] W. Kohn, Cyclotron resonance and de haas-van alphen oscillations of an interacting electron gas, Phys. Rev. **123**, 1242 (1961).
[39] S. Girvin, A. MacDonald, and P. Platzman, Magneto-roton theory of collective excitations in the fractional quantum hall effect, Phys. Rev. B **33**, 2481 (1986).
[40] This is analogous with the survival of the FQH state when perturbated by a periodic potential [44, 45], if in the FQAH case we consider deviation form the ideal trace condition as perturbation by a periodic potential.
[41] D. Antoniou and A. MacDonald, Magnetoplasmons and cyclotron resonance in disordered two-dimensional electronic systems, Phys. Rev. B **46**, 15225 (1992).
[42] A. Pinczuk, J. Valladares, D. Heiman, A. Gossard, J. English, C. Tu, L. Pfeiffer, and K. West, Observation of roton density of states in two-dimensional landau-level excitations, Phys. Rev. Lett. **61**, 2701 (1988).
[43] F. Wu, T. Lovorn, E. Tutuc, I. Martin, and A. MacDonald, Topological insulators in twisted transition metal dichalcogenide homobilayers, Phys. Rev. Lett. **122**, 086402 (2019).
[44] A. Kol and N. Read, Fractional quantum hall effect in a periodic potential, Phys. Rev. B **48**, 8890 (1993).
[45] D. Pfannkuche and A. H. MacDonald, Quantum hall effect of interacting electrons in a periodic potential, Phys. Rev. B **56**, R7100 (1997).